Optical quantum memory with optically inaccessible noble-gas spins

Or Katz,[1, 2, *] Eran Reches,[1] Roy Shaham,[1, 2] Alexey V. Gorshkov,[3] and Ofer Firstenberg[1]

[1] *Department of Physics of Complex Systems, Weizmann Institute of Science, Rehovot 76100, Israel*
[2] *Rafael Ltd, IL-31021 Haifa, Israel*
[3] *Joint Quantum Institute and Joint Center for Quantum Information and Computer Science,*
NIST/University of Maryland, College Park, Maryland 20742, USA

Optical quantum memories, which store and preserve the quantum state of photons, rely on a coherent mapping of the photonic state onto matter states that are optically accessible. Here we outline a new physical mechanism to map the state of photons onto the long-lived but optically inaccessible collective state of noble-gas spins. The mapping employs the coherent spin-exchange interaction arising from random collisions with alkali vapor. We analyze optimal strategies for high-efficiency storage and retrieval of non-classical light at various parameter regimes. Based on these strategies, we identify feasible experimental conditions for realizing efficient quantum memories with noble-gas spins having hours-long coherence times at room temperature and above.

Optical quantum memories enable the storage and retrieval of non-classical photonic signals. High performance memories are vital for various quantum-optics applications, including quantum communication, entanglement distribution, and universal quantum computation [1–5]. The memory storage duration is ultimately limited by the coherence time of the material state utilized by the memory [6]. Nuclear spins of rare isotopes of noble gases are enclosed by complete electronic shells and are thus well isolated from the environment. These spins feature hours-long lifetimes even when kept above room temperature [7, 8]. While not directly interacting with photons, these spins can be accessed via collisions with other, optically-accessible, atoms. A singular and challenging proposal from 2005, to utilize noble-gas spins for storage of squeezed-vacuum light, employs strong exchange collisions with meta-stable helium population sustained by electric discharge [9].

Recently a new mechanism for coherent coupling to noble-gas spins was identified, relying on weak spin-exchange collisions with alkali-metal atoms [10]. These collisions constructively accumulate to couple the collective quantum states of the noble-gas and alkali spins. The coupling is controllable and efficient at readily available experimental conditions. It enables the reversible transfer of quantum spin excitations, such as squeezed states, to and from the noble-gas spins [11].

In this Letter, we propose to use the spin-exchange interface for realizing a quantum memory, employing the alkali spins either as stepping-stones in a sequential process or as mediators in a single adiabatic process. By analyzing the dynamics in terms of collective canonical operators, we derive optimal control strategies for efficient mapping of the quantum state of an incoming light pulse onto the long-lived spin state of the noble gas. The schemes we identify, which circumvent the loss due to the shorter-lived alkali spins, are applicable to any physical four-level system with similar constrains. Fi-

nally, we present feasible experimental conditions for a quantum memory with helium-3.

The system we consider, shown in Fig. 1(a), comprises a noble gas mixed with alkali-metal vapor. The optical signal field $\hat{\mathcal{E}}$ interacts only with alkali atoms via the electric dipole interaction. Each alkali atom is modeled as a Λ system with two ground-level states $|\downarrow\rangle, |\uparrow\rangle$ and one excited state $|p\rangle$, as shown in Fig. 1(b). To simplify the intuitive explanation, we assume that $\hat{\mathcal{E}}$ is a single mode of a cavity and thus excites the symmetric, collective, optical dipole of all N_a alkali atoms $\hat{\mathcal{P}} \equiv \frac{1}{\sqrt{N_a}} \sum_a |\downarrow\rangle_a \langle p|_a$. A classical control field with Rabi frequency $\Omega(t)$ drives the $|p\rangle$–$|\uparrow\rangle$ transition, thereby coupling the signal field to the collective spin coherence $\hat{\mathcal{S}} \equiv \frac{1}{\sqrt{N_a}} \sum_a |\downarrow\rangle_a \langle\uparrow|_a$ of the alkali atoms [12]. This two-photon process circumvents the rapid decoherence of the optical dipole (*e.g.*, due to spontaneous emission or pressure broadening) and, by modulation of $\Omega(t)$, allows for the storage of the optical signal on and its retrieval from the spin $\hat{\mathcal{S}}$. At this point, $\hat{\mathcal{S}}$ may serve as a quantum memory whose lifetime is limited by the relaxation rate γ_s of the alkali spins [13–18]. We choose
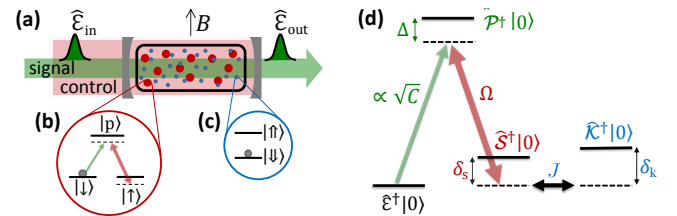
Figure 1. Optical quantum memory using noble-gas spins. (a) The input optical signal (green) is coherently mapped onto the collective state of noble-gas spins (blue) via collisions with alkali spins (red). (b) Modeled states of a polarized alkali atom. (c) Modeled states of a noble-gas atom. (d) Collective states of the alkali and noble-gas ensembles for a single input photon.

the states $|\downarrow\rangle$ and $|\uparrow\rangle$ such that $\hat{\mathcal{S}}$ is the annihilation operator of the total alkali spin, removing one quantum of spin from the alkali ensemble [19]. This choice subjects $\hat{\mathcal{S}}$ to coherent exchange with the noble-gas spins [10]. We consider N_b spin-1/2 noble-gas atoms with down and up spin states $|\Downarrow\rangle, |\Uparrow\rangle$, as shown in Fig. 1(c). These spins weakly interact with their surroundings, and their collective spin $\hat{\mathcal{K}} \equiv \frac{1}{\sqrt{N_b}} \sum_b |\Downarrow\rangle_b \langle\Uparrow|_b$, which we propose to employ as a quantum memory, has extremely low decoherence rate $\gamma_k \lll \gamma_s$.

The mapping of the optical signal onto the long-lived spin $\hat{\mathcal{K}}$ is mediated by multiple, weak, spin-exchange collisions between alkali and noble-gas atoms. The cumulative effect of these collisions is manifested as mutual exchange of collective spin excitations between the gases: $\{\partial_t \hat{\mathcal{S}}\}_{\text{ex}} = -iJ\hat{\mathcal{K}}$ and $\{\partial_t \hat{\mathcal{K}}\}_{\text{ex}} = -iJ\hat{\mathcal{S}}$. If the ensembles are highly polarized, particularly if all spins point downwards $|0\rangle = |\downarrow\rangle^{\otimes N_a} |\Downarrow\rangle^{\otimes N_b}$ in the absence of excitations, then the exchange rate of a single collective excitation is $J = \tilde{\zeta}\sqrt{N_a N_b}$, where $\tilde{\zeta}$ is a constant [10].

The collective quantum operators $\hat{\mathcal{P}}$, $\hat{\mathcal{S}}$, and $\hat{\mathcal{K}}$ are considered here in the rotating frame [12]. These operators satisfy the bosonic commutation relations and produce a single collective excitation when $\hat{\mathcal{P}}^\dagger$, $\hat{\mathcal{S}}^\dagger$, or $\hat{\mathcal{K}}^\dagger$ operate on the 'vacuum' state $|0\rangle$. Similarly, the input and output optical signals in a specific temporal mode are represented by the operators $\hat{\mathcal{E}}_{\text{in}}$, $\hat{\mathcal{E}}_{\text{out}}$ which satisfy the commutation relations $[\hat{\mathcal{E}}_{\text{in}}(t), \hat{\mathcal{E}}_{\text{in}}^\dagger(t')] = [\hat{\mathcal{E}}_{\text{out}}(t), \hat{\mathcal{E}}_{\text{out}}^\dagger(t')] = \delta(t - t')$.

The atom-photon interaction strength inside the cavity is parametrized by the cooperativity C, proportional to the product of the cavity finesse and the optical depth of the atomic medium [20, 21]. In the fast-cavity limit, the output field $\hat{\mathcal{E}}_{\text{out}}$ satisfies [12]

$$\hat{\mathcal{E}}_{\text{out}} = \hat{\mathcal{E}}_{\text{in}} + i\sqrt{2\gamma_p C}\hat{\mathcal{P}}, \qquad (1)$$

where γ_p denotes the dephasing rate of the atomic optical dipole, and $\gamma_p C$ corresponds to its stimulated emission rate.

In Ref. [22], we derive the equations of the atomic operators using the Bloch-Heisenberg-Langevin model. While the full equations are stochastic, the memory efficiency and bandwidth are governed by the deterministic part [23],

$$\partial_t \hat{\mathcal{P}} = -[\gamma_p(1 + C) + i\Delta]\hat{\mathcal{P}} + i\Omega\hat{\mathcal{S}} + i\sqrt{2\gamma_p C}\hat{\mathcal{E}}_{\text{in}}, \quad (2)$$

$$\partial_t \hat{\mathcal{S}} = -(\gamma_s + i\delta_s)\hat{\mathcal{S}} + i\Omega^*\hat{\mathcal{P}} - iJ\hat{\mathcal{K}}, \qquad (3)$$

$$\partial_t \hat{\mathcal{K}} = -(\gamma_k + i\delta_k)\hat{\mathcal{K}} - iJ\hat{\mathcal{S}}. \qquad (4)$$

Here Δ denotes the frequency detuning of the atomic optical transition from the cavity resonance, δ_s is the Raman (two-photon) detuning, and δ_k is the overall detuning of the full process. Figure 1(d) shows the corresponding four-level diagram for the simple but quintessential case of a single-photon signal.

We aim to find a controllable and reversible process that efficiently transfers the quantum excitations from $\hat{\mathcal{E}}_{\text{in}}$ to $\hat{\mathcal{K}}$ and then back from $\hat{\mathcal{K}}$ to $\hat{\mathcal{E}}_{\text{out}}$. Controlling the exchange $\hat{\mathcal{E}} \leftrightarrow \hat{\mathcal{P}} \leftrightarrow \hat{\mathcal{S}}$ is done externally by varying the control field $\Omega(t)$. However, the same cannot be done for $\hat{\mathcal{S}} \leftrightarrow \hat{\mathcal{K}}$, as the collisional coupling J is constant. Instead, one can externally vary the $\hat{\mathcal{S}} \leftrightarrow \hat{\mathcal{K}}$ frequency mismatch $\delta \equiv \delta_k - \delta_s = \delta[B(t)]$, given by the difference in spin precession frequencies of the two species, which linearly depends on the bias magnetic field $B(t)$. Intuitively, the exchange $\hat{\mathcal{S}} \leftrightarrow \hat{\mathcal{K}}$ is enabled when $B(t)$ is tuned to resonance ($\delta = 0$) and is suppressed away from resonance.

We assume an input pulse with typical duration T and bandwidth $1/T$, containing $N = \int_{-\infty}^T dt \langle\hat{\mathcal{E}}_{\text{in}}^\dagger(t)\hat{\mathcal{E}}_{\text{in}}(t)\rangle$ photons. We search for the temporal shapes of $\Omega(t)$, $\delta(t)$ and $\delta_s(t)$ that maximize the storage efficiency $\eta = \langle\hat{\mathcal{K}}^\dagger\hat{\mathcal{K}}\rangle/N$, where $\langle\hat{\mathcal{K}}^\dagger\hat{\mathcal{K}}\rangle$ is the number of noble-gas excitations after storage. From here on, we focus on the relevant regime of strong atom-photon coupling $\gamma_p CT \gg 1$, where the optical dipole $\hat{\mathcal{P}}$ follows $\hat{\mathcal{E}}_{\text{in}}$ and $\hat{\mathcal{S}}$ and can be adiabatically eliminated [12, 22]. We can then safely take $\Delta = 0$ while maintaining $\langle\hat{\mathcal{P}}^\dagger\hat{\mathcal{P}}\rangle \ll 1$.

We adopt the optimal-control tools developed for a standard three-level memory [24]. We solve Eqs. (2-4) with an input optical signal $\langle\hat{\mathcal{E}}(t)^\dagger\hat{\mathcal{E}}(t)\rangle = A\sqrt{2/T}e^{(t-T)/T}$ for $-2T \leq t \leq T$, where A guarantees the pulse contains a single photon. We then iterate on $\Omega(t)$, $\delta(t)$, and $\delta_s(t)$ using the gradient ascent method [22]. The optimization calculations for given J, γ_s, and T are done with no relaxation of the noble-gas spins $\gamma_k = 0$ (since $\gamma_k \lll 1/T$) and with cooperativity $C \gg 1$, yielding the ideal storage efficiency η_∞. Finite cooperativity will lower the storage efficiency to $\eta = (\frac{C}{C+1})\eta_\infty$, as well as the total memory efficiency (storage and retrieval) which is approximately given by η^2 [12, 22].

For a sufficiently long pulse ($T \gg 1/J$) or in the absence of alkali relaxation ($\gamma_s = 0$), we recover as expected the ideal result of the three-level memory: $\eta_\infty \to 1$ and $\eta = \frac{C}{C+1}$ [12]. Furthermore, we find that the mapping is optimal when the two-photon transition is tuned on resonance $\delta_s(t) = 0$ [22]. However for finite γ_s and T, the memory operation depends on two additional parameters $\gamma_s T$ and J/γ_s, and indeed we reveal qualitatively-different optimal solutions. The optimal efficiencies, shown in Fig. 2(a), approach unity when the spins are strongly coupled ($J \gg \gamma_s$) or when the input pulses are long ($T \gg 1/J, \gamma_s/J^2$). These regimes correspond to two distinct storage schemes, presented in Fig. 3 and exemplified in Fig. 4.

For short signal pulses $T \ll 1/\gamma_s$ and $T \lesssim 1/J$ in the strong-coupling regime [Figs. 3(bottom) and 4(a)],
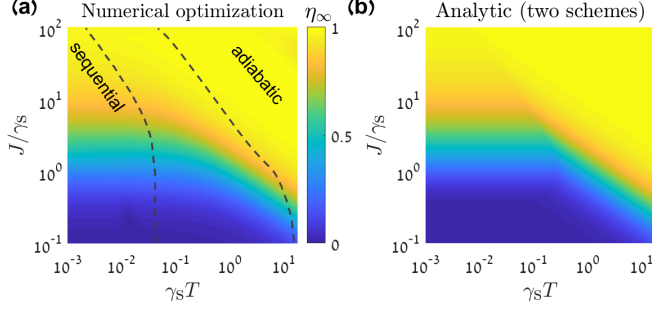
Figure 2. Optimal storage efficiency η_∞ obtained from (a) the gradient ascent optimization and compared to (b) the analytic prediction for the sequential and adiabatic schemes. The efficiency approaches unity when the coupling strength J between the alkali and noble-gas spins increases (compared to the alkali relaxation rate γ_s), and when the pulse duration T increases. The actual efficiency $\eta = \frac{C}{C+1}\eta_\infty$ depends also on the atom-photon cooperativity C. We associate an optimal solution with the sequential scheme if the single input excitation is first predominately stored on the alkali spin $\langle \hat{S}^\dagger(T)\hat{S}(T)\rangle \geq 0.95$ and only later transferred to the noble-gas spin. We associate a solution with the adiabatic scheme if $\langle \hat{S}^\dagger(t)\hat{S}(t)\rangle \leq 0.05$ throughout the process. The dashed lines in (a) mark the boarders of these regimes.

a sequential scheme is optimal, where the alkali spins are used as a temporary memory before transferring the excitations to the noble-gas spins. For long pulses [Figs. 3(top) and 4(b)], an adiabatic scheme is optimal, where the excitation goes directly to the noble-gas spins, and the alkali spins act as mediators that adiabatically follow. We provide below an analytic description for the two schemes, and their efficiencies in the relevant limits for exponentially-shaped signals. The efficiencies are also given in Fig. 3 and can be intuitively understood in terms of the competition between the relaxation rates γ_p, γ_s, γ_k and the respective stimulated rates $C\gamma_p$, γ_Ω, γ_J as given in the figure.

We begin with short pulses $T \ll 1/\gamma_s$ in which the sequential scheme is optimal. In the first stage, the input field $\hat{\mathcal{E}}_{in}$ is mapped onto the alkali spins $\hat{S}(T)$ while the noble-gas spins are decoupled by $\delta \gg J$. The standard three-level mapping is given by [12]

$$\hat{S}(T) = \int_{-\infty}^{T} h_\Omega(t)\hat{\mathcal{E}}_{in}(t)dt. \qquad (5)$$

The function $h_\Omega(t) = a_\Omega(t)\exp[-\int_t^T(\gamma_s + \gamma_\Omega)dt']$ depends on the stimulated-coupling rate $\gamma_\Omega \equiv |\Omega|^2/[\gamma_p(C+1)]$ and on $a_\Omega = -\sqrt{2\gamma_p C \gamma_\Omega}/\Omega$. Efficiency is maximized upon optimizing the temporal form of the control field $\Omega(t)$ such that $h_\Omega^*(t)$ follows the complex amplitude of the incoming pulse [12, 25–27]. For the exponentially-shaped input signal we consider, the optimal control field $\Omega(t)$ is approximately constant. In
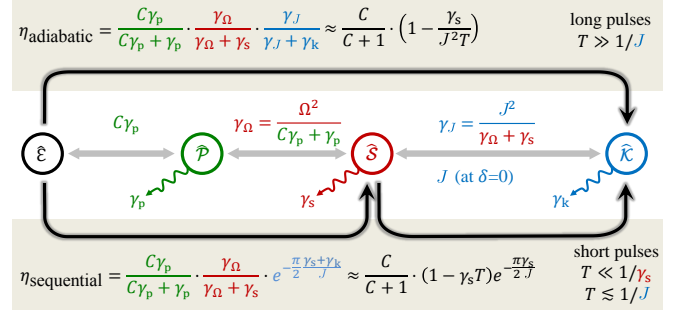

Figure 3. Optimal mapping schemes of an optical signal $\hat{\mathcal{E}}$ onto a long-lived coherence $\hat{\mathcal{K}}$ (noble-gas spin) via short-lived coherences $\hat{\mathcal{P}}$ and $\hat{S}$ (alkali optical dipole and alkali spin, respectively). The fully-adiabatic scheme (top) is optimal for long optical pulses. The respective mapping efficiency $\eta_{adiabatic}$ approaches 1 when the relaxation rates γ_p, γ_s, $\gg \gamma_k$ are small compared to the corresponding stimulated coupling rates $C\gamma_p$, γ_Ω, γ_J. A sequential scheme (bottom) is optimal for short optical pulses. Here an adiabatic mapping of $\hat{\mathcal{E}}$ onto $\hat{S}$, as in standard light storage, is followed by tuning $\hat{S}$ and $\hat{\mathcal{K}}$ to a resonant exchange ($\delta = 0$). The respective mapping efficiency $\eta_{sequential}$ comprises the efficiencies of both stages and can approach 1 when $\hat{S}$ and $\hat{\mathcal{K}}$ are strongly coupled (i.e., when $J \gg \gamma_s$, where J is the collective spin-exchange rate). Setting $\gamma_\Omega = 1/T - \gamma_s$ for retrieval of an exponentially-shaped pulse in the sequential scheme, or $\gamma_\Omega = TJ^2 - \gamma_s$ (i.e., $\gamma_J = 1/T$) for the adiabatic scheme, we obtain the expressions in black, which also provide a rough approximation for a general signal with duration $\sim T \ll 1/\gamma_k$ and bandwidth $\sim 1/T$.

the second stage, the control field is turned off, and the collisional coupling between the collective alkali and noble-gas spins is tuned to resonance [$\delta(B) = 0$] for the duration $T' - T = \pi/(2J)$ for $J \gg \gamma_s$. This maximizes the coherent transfer of the excitation, $\hat{\mathcal{K}}(T') \approx e^{-\pi\gamma_s/(4J)}\hat{S}(T)$. This scheme features the same bandwidth $T^{-1} \lesssim \gamma_\Omega$ as alkali-based memories, increasing with the control power. The efficiency $\eta_{sequential}$, presented in Fig. 3, approaches unity for large cooperativity ($C \gg 1$), strong spin-exchange coupling ($J \gg \gamma_s$), and strong control field ($\gamma_\Omega \gg \gamma_s$).

We now turn to the regime of long pulses $T \gg 1/J$, where the adiabatic scheme is optimal. Remarkably, here the input field $\hat{\mathcal{E}}_{in}$ is mapped directly onto the noble-gas spins $\hat{\mathcal{K}}(T)$, keeping the alkali spins unexcited $\langle \hat{S}^\dagger \hat{S}\rangle \ll 1$. The collisional coupling is tuned to resonance [$\delta(B) = 0$] from the onset, effectively hybridizing $\hat{S}$ and $\hat{\mathcal{K}}$. For $\gamma_\Omega \gg J$, the alkali spin $\hat{S}$ adiabatically follows $\hat{\mathcal{E}}_{in}$ and $\hat{\mathcal{K}}$, satisfying $\hat{S} = i(a_J\hat{\mathcal{E}}_{in} - \gamma_J\hat{\mathcal{K}})/J$, where $\gamma_J = J^2/(\gamma_\Omega + \gamma_s)$ is the stimulated-coupling rate to the noble-gas spin, and $a_J = ia_\Omega\gamma_J/J$. Substituting this state in Eq. (4) yields the linear mapping between
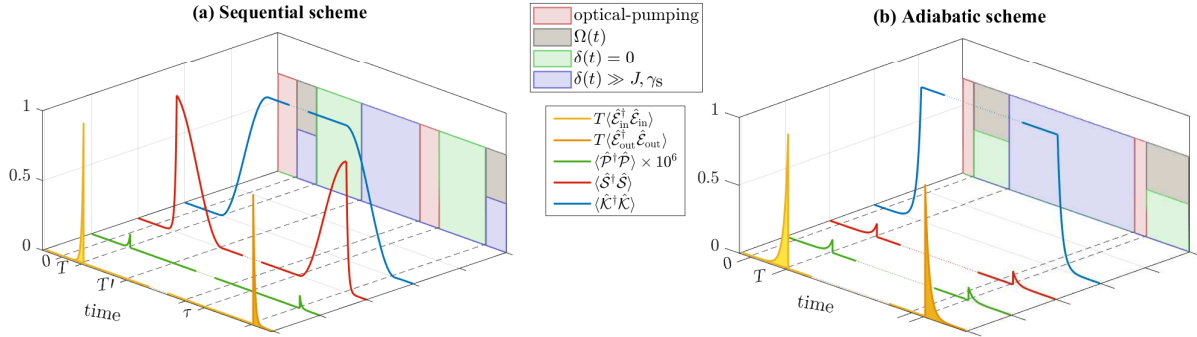
Figure 4. Numerical calculations of optimal storage and retrieval for a polarized potassium\helium-3 mixture at feasible experimental conditions. (a) High-bandwidth memory of a short ($T = 15\,\mu$s) single-photon pulse. The input pulse (yellow) is first mapped onto the collective alkali spin (red) employing standard 3-level storage and then transferred to the collective noble-gas spin (blue). (b) Memory in the adiabatic regime of a long ($T = 15\,$ms) single-photon pulse. The input pulse is mapped directly onto the collective noble-gas spin, by only virtually exciting the alkali spins. The total memory efficiency is $\eta^2 = 0.93$ for the sequential scheme and $\eta^2 = 0.97$ for the adiabatic scheme at the proposed experimental conditions.

the optical signal and the noble-gas spins

$$\hat{\mathcal{K}}(T) = \int_{-\infty}^{T} h_J(t)\hat{\mathcal{E}}_{\text{in}}(t)dt, \qquad (6)$$

where $h_J(t) = a_J(t)\exp\big(-\int_t^T[\gamma_{\text{k}}+\gamma_J]dt'\big)$. Maximal efficiency is again achieved upon optimal shaping of $\Omega(t)$ such that now it is $h_J^*(t)$ that follows the complex amplitude of the incoming pulse. The memory bandwidth is now reduced to approximately $T^{-1} \lesssim \gamma_J$. The storage efficiency $\eta_{\text{adiabatic}}$ is presented in Fig. 3 for a constant γ_Ω and $2T = 1/\gamma_J$. The efficiency approaches unity for large cooperativity ($C \gg 1$) and strong control field ($\gamma_\Omega \gg \gamma_{\text{s}}$).

To illustrate the competition between the sequential and adiabatic schemes, we present $\max\{\eta_{\text{adiabatic}}, \eta_{\text{sequential}}\}$ in Fig. 2(b). We use the analytic expressions from Fig. 3, with $\gamma_\Omega \to \infty$ for the sequential scheme and $\gamma_\Omega = J^2 T$ for the adiabatic scheme, which maximizes $\eta_{\text{sequential}}$ within the bandwidth constraints. Interestingly, the analytic results provide a good approximation to the optimal efficiency [Fig. 2(a)] even away from their validity limits ($J \gg \gamma_{\text{s}}$ or $T \gg 1/J$).

During the long memory time, the collective noble-gas spin is susceptible to alkali-induced relaxation $\gamma_J = J^2\gamma_{\text{s}}/(\gamma_{\text{s}}^2 + \delta^2)$. Fortunately, it is possible to effectively decouple the two spins following the storage process by either applying a large magnetic field $\delta(B) \gg J\sqrt{\gamma_{\text{s}}/\gamma_{\text{k}}}$ or by letting the alkali atoms depolarize. Finally as shown in Fig. 4, retrieval of a signal with the same typical duration T can be realized by time-reversing the storage sequence [12, 25, 28].

Our model uses only two states, $|\!\downarrow\rangle$ and $|\!\uparrow\rangle$, to represent the alkali spin. Real alkali atoms, however, possess more spin states due to the nonzero nuclear spin I > 1/2. Among these states, $|\!\downarrow\rangle$ and $|\!\uparrow\rangle$ are chosen so as to enable the coherent exchange with the noble-gas spin via collisions. Between collisions, the strong hyperfine interaction renders the total alkali spin $\text{F} = \text{I} \oplus \text{S}$ a good quantum number. However during a collision, only the electron spin of the alkali atom ($\text{S} = 1/2$) interacts with the nuclear spin of the noble-gas atom ($\text{K}=1/2$), exchanging not more than one unit of spin [29, 30]. Efficient exchange of spin excitations is thus possible if the difference between $|\!\downarrow\rangle$ and $|\!\uparrow\rangle$ is a single unit of spin, and the excitation is encoded on the orientation (first moment) of the total alkali spin [31]. An optical Λ-type coupling to the alkali spin orientation is possible even at high noble-gas pressures [5, 26, 32]. Consequently, for highly polarized alkali spins, $|\!\downarrow\rangle$ and $|\!\uparrow\rangle$ are both in the $F = I + 1/2$ hyperfine manifold, and their spin projection along the polarization axis are $I + 1/2$ and $I - 1/2$, respectively. This particular combination of states is also free from relaxation by alkali-alkali spin-exchange collisions [19, 33].

Before concluding, we analyze an experimental configuration in which the proposed memory schemes can be realized. We consider a mixture of potassium and helium-3, enclosed in a spherical glass cell with a 1 cm radius. We take helium-3 density of $n_{\text{b}} = 2 \cdot 10^{20}\,\text{cm}^{-3}$ (7.5 atm at ambient conditions), potassium density of $n_{\text{a}} = 3.5 \cdot 10^{14}\,\text{cm}^{-3}$ (220°C), and 30 Torr of N_2 to mitigate radiation trapping. The alkali spins can be initialized using standard optical-pumping, reaching high spin-polarization $p_{\text{a}} \geq 95\%$ [29], and the noble-gas spins can be initialized via spin-exchange optical-pumping, reaching $p_{\text{b}} \gtrsim 75\%$ hyperpolarization [8, 34]. As long as magnetic-field inhomogenities are minimized, the noble-gas spin state can exhibit coherence times of up to $1/\gamma_{\text{k}} = 100$ hours, limited by self dipole-dipole inter-

actions [8, 35]. These parameters yield $J = 1000\ \text{s}^{-1}$ and $\gamma_{\text{s}} = 17\ \text{s}^{-1}$ for the lowest-order diffusion mode [36, 37], and an optical cooperativity of $C \approx 100$ [22]. The memory operates in the regime known as SERF (spin-exchange relaxation free), and therefore γ_{s} is unaffected by rapid spin-exchange collisions of alkali-atom pairs [19, 33, 38, 39].

Any nonclassical state of light, such as squeezed states and single photons, can be stored in the proposed memory. To illustrate this, we present in Fig. 4 calculations of storage and retrieval of a single photon, at the above physical conditions, with $\gamma_{\Omega} = 10^4\ \text{s}^{-1}$. We obtain a total memory efficiency (storage and retrieval) of $\eta^2 \approx 0.93$ for a $T = 15\,\mu\text{s}$ input pulse with the sequential storage scheme, and an efficiency of $\eta^2 \approx 0.97$ for a $T = 15\,\text{ms}$ input pulse with the adiabatic scheme.

In conclusion, we present a model for a hybrid system comprising light and an ensemble of collisionally-coupled spins and identify reversible and efficient processes for mapping the photons onto the optically inaccessible spins. Although we solve the cavity model, we expect that, in the fast-cavity limit we consider, it also captures the main features of a free-space realization. A fully adiabatic process is optimal for long pulses, while a sequential process prevails for short pulses. These processes enable on-demand storage and retrieval of quantum states of light onto noble-gas spins at feasible experimental conditions. This work lays the groundwork for applications of noble-gas spins in optical quantum memories with potentially hours-long storage times.

---

* Corresponding author:or.katz@weizmann.ac.il

[1] A. I. Lvovsky, B. C. Sanders & W. Tittel, Nature Photon. 3, 706–714 (2009).
[2] J. L. O'Brien, Science 318, 1567–1570 (2007).
[3] K. Heshami, D. G. England, P. C. Humphreys, P. J. Bustard, V. M. Acosta, J. Nunn & B. J. Sussman, J. Mod. Opt. 63, 2005–2028 (2016).
[4] N. Sangouard, C. Simon, H. deRiedmatten & N. Gisin, Rev. Mod. Phys. 83, 33–80 (2011).
[5] K. Hammerer, A. S. Sørensen & E. S. Polzik, Rev. Mod. Phys. 82, 1041–1093 (2010).
[6] I. Novikova, R. Walsworth & Y. Xiao, Laser Photon. Rev. 6, 333–353 (2012).
[7] C. Gemmel, et al. Eur. Phys. J. D 57, 303 (2010).
[8] T. R. Gentile, P. J. Nacher, B. Saam & T. G. Walker, Rev. Mod. Phys. 89, 045004 (2017).
[9] A. Dantan, G. Reinaudi, A. Sinatra, F. Laloë, E. Giacobino & M. Pinard, Phys. Rev. Lett. 95, 123002 (2005).
[10] O. Katz, R. Shaham & O. Firstenberg, arXiv preprint arXiv:1905.12532 (2019).
[11] O. Katz, R. Shaham, E. S. Polzik, and O. Firstenberg, Phys. Rev. Lett. 124, 043602 (2020).
[12] A. V. Gorshkov, A. André, M. D. Lukin & A. S. Sørensen, Phys. Rev. A 76, 033804 (2007).
[13] D. F. Phillips, A. Fleischhauer, A. Mair, R. L. Walsworth, and M. D. Lukin, Phys. Rev. Lett. 86, 783–786 (2001).
[14] M. D. Lukin, Rev. Mod. Phys. 75, 457–472 (2003).
[15] M. Hosseini, B. M. Sparkes, G. Campbell, P. K. Lam & B. C. Buchler, Nat. Commun. 2, 174 (2011).
[16] B. Julsgaard, J. Sherson, J. I. Cirac, J. Fiurášek & E. S. Polzik, Nature 432, 482–486 (2004).
[17] K. Jensen, W. Wasilewski, H. Krauter, T. Fernholz, B. M. Nielsen, M. Owari, M. B. Plenio, A. Serafini, M. M. Wolf & E. S. Polzik, Nature Phys. 7, 13–16 (2011).
[18] D. J. Saunders, J. H. D. Munns, T. F. M. Champion, C. Qiu, K. T. Kaczmarek, E. Poem, P. M. Ledingham, I. A. Walmsley & J. Nunn. Phys. Rev. Lett. 116, 090501 (2016).
[19] O. Katz & O. Firstenberg, Nat. Commun. 9, 2074 (2018).
[20] O. Lahad & O. Firstenberg, Phys. Rev. Lett. 119, 113601 (2017).
[21] A. V. Gorshkov, A. André, M. D. Lukin & A. S. Sørensen., Phys. Rev. A 76, 033805 (2007).
[22] O. Katz, R. Shaham, E. Reches, A. V. Gorshkov & O. Firstenberg. To be published.
[23] The stochastic part is mainly responsible for the preservation of commutation relations through introduction of vacuum noise [5, 10, 12].
[24] A. V. Gorshkov, T. Calarco, M. D. Lukin & A. S. Sørensen, Phys. Rev. A 77, 043806 (2008).
[25] A. V. Gorshkov, A. André, M. Fleischhauer, A. S. Sørensen & M. D. Lukin. Phys. Rev. Lett. 98, 123601 (2007).
[26] J. Sherson, A. S. Sørensen, J. Fiurášek, K. Mølmer & E. S. Polzik. Phys. Rev. A 74, 011802(R) (2006).
[27] M. D. Lukin, S. F. Yelin, and M. Fleischhauer , Phys. Rev. Lett. 84, 4232 (2000).
[28] I. Novikova, A.V. Gorshkov, D.F. Phillips, A.S. Sørensen, M.D. Lukin, and R.L. Walsworth, Phys. Rev. Lett. 98, 243602 (2007).
[29] W. Happer, Y. Y. Jau & T. Walker, Optically pumped atoms. 159–218 (WILEY-VCH Press, 2010).
[30] T. W. Kornack & M. V. Romalis, Phys. Rev. Lett. 89, 253002 (2002).
[31] M. Auzinsh, D. Budker & S. M. Rochester, Phys. Rev. A 80, 053406 (2009).
[32] C. A. Muschik, K. Hammerer, E. S. Polzik & J. I. Cirac,

Phys. Rev. A 73 062329 (2006).

[33] W. Happer & A. C. Tam, Phys. Rev. A 16, 1877 (1977).

[34] T. G. Walker & W. Happer, Rev. Mod. Phys. 69, 629–642 (1997).

[35] G. D. Cates, S. R. Schaefer & W. Happer. Phys. Rev. A 37, 2877 (1988).

[36] S. Kadlecek, T. Walker, D. K. Walter, C. Erickson, and W. Happer. Phys. Rev. A 63, 052717 (2001).

[37] R. Shaham, O. Katz, and O. Firstenberg, arXiv preprint arXiv:2006.04243 (2020).

[38] O. Katz, M. Dikopoltsev, O. Peleg, M. Shuker, J. Steinhauer, and N. Katz. Phys. Rev. Lett. 110, 263004 (2013).

[39] J. Kong, R. Jiménez-Martínez, C. Troullinou, V. G. Lucivero & M. W. Mitchell, arXiv preprint arXiv:1804.07818 (2018).